Solid-State NMR Characterization of Polysiloxane Matrixes Functionalized with Ether−Phosphines and Their Ruthenium(II) and Palladium(II) Complexes[1]

Ekkehard Lindner,* Rudolf Schreiber, Martin Kemmler, Theodor Schneller, and Hermann A. Mayer

Institut für Anorganische Chemie der Universität, Auf der Morgenstelle 18, D-72076 Tübingen, Germany

Received December 13, 1994. Revised Manuscript Received February 13, 1995[⊗]

The monomeric ether−phosphine ligand $(MeO)_3Si(CH_2)_3(Ph)PCH_2CH_2OMe$ [$\mathbf{1(T^0)}$] and its P-coordinated trimethoxysilyl-(T)-functionalized ruthenium and palladium complexes HRuCl(CO)(P~O)$_3$ [$\mathbf{2(T^0)_3}$] and $Cl_2Pd(P{\sim}O)_2$ [$\mathbf{3(T^0)_2}$] were sol−gel processed with variable amounts of $MeSi(OMe)_3$ ($\mathbf{T^0}$) and $Me_2Si(OEt)_2$ ($\mathbf{D^0}$) to give the polysiloxane-bound ether−phosphine ligands [$\mathbf{1(T^n)(D^i)_y}$], [$\mathbf{1(T^n)(T^m)_2}$], the ruthenium complexes [$\mathbf{2(T^n)_3(D^i)_y}$], [$\mathbf{2(T^n)_3(T^m)_y}$], and [$\mathbf{2(T^n)_3(T^m_{PMS})_y}$], and the palladium complexes [$\mathbf{3(T^n)_2(D^i)_y}$] (Table 1) {P~O: η^1-P-coordinated ether−phosphine ligand; $(T^{n,m})_y$, $(D^i)_y$: y = number of co-condensated T type (three oxygen neighbors), D type (two oxygen neighbors) silicon atom; n, m, i = number of Si−O−Si bonds; $n, m = 0-3$; $i = 0-2$; PMS = polymethylsiloxane; $\mathbf{1(T^n)(D^i)_y}$: $[F-SiO_{n/2}(OX)_{3-n}][Me_2SiO_{i/2}(OX)_{2-i}]_y$, X = H, Me, Et; F = $(Ph)P(CH_2CH_2OMe)(CH_2)_3-$ (**1**), $\mathbf{1(T^n)(T^m)_2}$: $[F-SiO_{n/2}(OX)_{3-n}][MeSiO_{m/2}(OX)_{3-m}]_2$; $\mathbf{2(T^n)_3(D^i)_y}$: $[F-SiO_{n/2}(OX)_{3-n}]_3[Me_2SiO_{i/2}(OX)_{2-i}]_y$, F = $[HRuCl(CO)]_{1/3}(Ph)P(CH_2CH_2OMe)(CH_2)_3-$ (**2**); $\mathbf{3(T^n)_2(D^i)_y}$: $[F-SiO_{n/2}(OX)_{3-n}]_2[Me_2SiO_{i/2}(OX)_{2-i}]_y$, F = $(Cl_2Pd)_{1/2}(Ph)P(CH_2CH_2OMe)(CH_2)_3-$ (**3**); $\mathbf{2(T^n)_3(T^m)_y}$, $\mathbf{2(T^n)_3(T^m_{PMS})_y}$: $[F-SiO_{n/2}(OX)_{3-n}]_3[MeSiO_{m/2}(OX)_{3-m}]_2$}. ^{29}Si CP MAS NMR spectroscopic investigations showed that there is an upper limit for the molar amount of y of the D^i units in the compounds $\mathbf{1(T^n)(D^i)_y}$, $\mathbf{2(T^n)_3(D^i)_y}$, and $\mathbf{3(T^n)_2(D^i)_y}$. The degree of condensation of the silicon units in $\mathbf{2(T^n)_3(T^m)_y}$ depends on the amount of y of the $\mathbf{T^m}$ co-condensate. The line widths of the signals in the ^{31}P CP MAS NMR spectra suggest that the phosphorus atom of $\mathbf{1(T^n)(D^i)_y}$ has a very high mobility in comparison to the ligands $\mathbf{1(T^n)(T^m)_2}$ and $[F-SiO_{n/2}(OX)_{3-n}][SiO_{k/2}(OX)_{4-k}]_2$ [$\mathbf{1(T^n)(Q^k)_2}$] [F = **1**, Q^k: Q type (four oxygen neighbors) silicon atom; k = 0−4, number of Si−O−Si bonds], and to the ruthenium complexes $\mathbf{2(T^n)_3(T^m)_y}$. This was confirmed by the relaxation times in the rotating frame $T_{1\varrho H}$ and the cross polarization parameters T_{XH} (X = Si, P). It is concluded from T_{SiH} and $T_{1\varrho H}$ (via ^{29}Si) data that the polysiloxane matrix becomes more flexible if $\mathbf{D^0}$ units are used as the co-condensate. The polymeric materials $\mathbf{2(T^n)_3(T^m)_y}$ are built up homogeneously for $y = 0-48$ on a scale of 3 nm. The $T_{1\varrho H}$ relaxation time was found to depend on the amount of y of the co-condensate. In the cases of $y = 96$ and of $\mathbf{2(T^n)_3(T^m_{PMS})_y}$ an interruption of the spin diffusion process was found, which indicates the formation of several aggregates. The spin diffusion rate was used to estimate a characteristic spin diffusion distance of 1.8 to 3 nm for $y = 0-48$, employing a model diffusion equation.

Introduction

Recently techniques have gained increasing significance in which the reactive center which is responsible for chemical reactions is supported. An excellent method of the synthesis of suitable polymers offers the sol−gel process.[2] Hydrolysis and polycondensation of organosilylalkoxides $RSi(OR')_3$ with stable silicon-carbon bonds enable a simple, mild, and low-temperature synthesis for polymer frameworks:[3,4]

$$n\mathrm{RSi(OR')_3} \xrightarrow[\mathrm{[-R'OH]}]{\mathrm{[H_2O]}} [\mathrm{RSiO_{3/2}}]_n$$

Even potentially catalytic active organometallic complexes can be incorporated in such systems, if they are provided with organofunctional silyl−(T−) groups.[5-9] In particular the simultaneous co-condensation of organo−(T−) functionalized transition metal complexes with D−, T−, or Q−alkoxysilanes [$D = R_2Si(OR')_2$, $T = RSi(OR')_3$, $Q = Si(OR')_4$; R, R' = Me, Et] affords the possibility to modify these inorganic−organic hybrid materials. These

---

[⊗] Abstract published in *Advance ACS Abstracts*, April 1, 1995.

(1) Supported Organometallic Complexes Part 7. Part 6: Lindner, E.; Kemmler, M.; Mayer, H. A. *Z. Anorg. Allg. Chem.* **1994**, *620*, 1142.

(2) Brinker, C. J.; Scherer, G. W. *Sol Gel Science*; Academic Press: London, 1990.

(3) Corriu, R. J. P.; Moreau, J. J. E.; Thepot, P.; Wong Chi Man, M.; Chorro, C.; Lere-Porte, J.-P.; Sauvajol, J.-L. *Chem. Mater.* **1994**, *6*, 640.

(4) Shea, K. J.; Loy, D. A.; Webster, O. *J. Am. Chem. Soc.* **1992**, *114*, 6701.

(5) Breitscheidel, B.; Zieder, J.; Schubert, U. *Chem. Mater.* **1991**, *3*, 559.

(6) Schubert, U.; Amberg-Schwab, S.; Breitscheidel, B. *Chem. Mater.* **1989**, *1*, 576.

(7) Egger, C.; Schubert, U. *Z. Naturforsch.* **1991**, *46 Part B*, 783.

(8) Lindner, E.; Kemmler, M.; Mayer, H. A.; Wegner, P. *J. Am. Chem. Soc.* **1994**, *116*, 348.

(9) Lindner, E.; Bader, A.; Glaser, E.; Pfleiderer, B.; Schumann, W.; Bayer, E. *J. Organomet. Chem.* **1988**, *355*, 45.

0897-4756/95/2807-0951$09.00/0

novel two- or three-dimensional networks have superior mechanical and chemical properties.[1] In addition, these frameworks are considered to be stationary phases, which can be penetrated by a mobile phase such as solvents, gases, or reactants. Although the penetration takes place in molecular dimensions no homogeneous mixture but an interphase is formed.[8-12] The most important advantages of such complexes bound to a polysiloxane matrix are (i) easy and complete separation of the reacted substrates from the polymer, (ii) the reaction centers in the stationary phase are well accessible for the reactants in the mobile phase, (iii) the density and distance of the reactive centers are controllable and thus the *reactivity* can be adjusted, (iv) depending on different requirements, the polymer as well as the spacer can be designed either more rigid or more flexible; the *selectivity* of the reactions therefore is controllable, (v) finally the leaching is reduced, in particular in the case of polyfunctionalized ligands and complexes.

In a previous paper[8] we were able to demonstrate, that the distribution of the organometallic complexes within the functionalized T/Q polymers depends on the stoichiometry and the conditions of the condensation reactions. A decrease of the T/Q ratio may result in the formation of domains enriched with Q groups, which is accompanied by a simultaneous reduction of the catalytic activity. In continuation of this work, we set out to examine whether T/T and T/D mixtures show also a tendency to build up areas where the enrichment of one of this species is preferred. The study of this mixing on the molecular level of the T-functionalized ether–phosphine complexes $HRuCl(CO)(P{\sim}O)_3$ **[2(T^n)$_3$]** and $Cl_2Pd(P{\sim}O)_2$ **[3(T^n)$_2$]** [P~O: η^1-P-coordinated $PhP(CH_2CH_2OMe)(CH_2)_3SiO_{n/2}(OX)_{3-n}$ ligand] with the matrix components $MeSiO_{m/2}(OX)_{3-m}$ **(T^m)** and $Me_2SiO_{i/2}(OX)_{2-i}$ **(D^i)** (X = H, Me, Et; $m, n = 0-3$; $i = 0-2$) is the main objective of the present article. Moreover, we want to synthesize stationary phases for the use in interphase systems.

To characterize the T/T and T/D blends heteronuclear solid-state NMR spectroscopy was employed. The stereochemistry of the metal complexes, the integrity of the spacers and the ligand backbone was established by ^{31}P and ^{13}C CP MAS NMR spectroscopy, respectively. For the quantification of the different silyl species and the determination of the degree of hydrolysis and condensation of the T and D groups silicon-29 and carbon-13 solid-state NMR investigations were carried out.

Results and Discussion

Sol–Gel Processing. Three methods were found to be applicable to the hydrolysis, polycondensation, and co-condensation of the already known monomeric ether–phosphine ligand $PhP(CH_2CH_2OMe)(CH_2)_3Si(OMe)_3$ **[1(T^0)]** and its ruthenium and palladium complexes $HRuCl(CO)(P{\sim}O)_3$ **[2(T^0)$_3$]** and *cis/trans*-$Cl_2Pd(P{\sim}O)_2$ **[3(T^0)$_2$]** (P~O: η^1-P-coordinated ether–phosphine ligand, Scheme 1) with $MeSi(OMe)_3$ **(T^0)** and $Me_2Si(OEt)_2$ **(D^0)**, respectively.

According to method 1 the monomeric starting compounds were mixed with $MeSi(OMe)_3$ **(T^0)** or $Me_2Si(OEt)_2$ **(D^0)** in the presence of the catalyst, and an excess of water without any further solvent. In the case of method 2 the monomeric precursor was polycondensated with water in the presence of the catalyst as reported in the literature.[13] The resulting polycondensate was co-condensated in a second step with $MeSi(OMe)_3$ **(T^0)** under the same reaction conditions as in method 1 (method 2). If the starting compound is only slightly soluble in alcohols, additional alcohol is necessary for the polycondensation, which was carried out in the presence of water, $Me_2Si(OEt)_2$ **(D^0)**, and the catalyst (method 3).

Scheme 1[a]

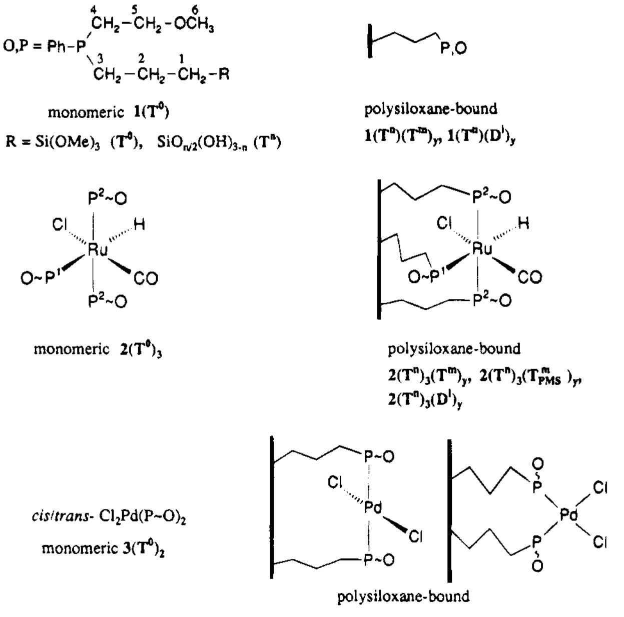

[a] i, m, n = number of Si–O–Si bonds ($n, m = 0-3$; $i = 0-2$). y = number of co-condensated T, D silicon atoms. P~O: η^1-P-coordinated ether–phosphine ligand $PhP(CH_2CH_2OMe)(CH_2)_3Si(OMe)_3$ and $PhP(CH_2CH_2OMe)CH_2CH_2CH_2SiO_{n/2}(OH)_{3-n}$, respectively. PMS: T-type polymethylsiloxane, prepared according to method 2; see also Experimental Section. $T^{m,n}$: T type silicon atom (three oxygen neighbors). D^i: D type silicon atom (two oxygen neighbors).

Method 1 has been applied to the synthesis of the polymeric ligands $[F-SiO_{n/2}(OX)_{3-n}][MeSiO_{m/2}(OX)_{3-m}]_y$ **[1(T^n)(T^m)$_2$]** and $[F-SiO_{n/2}(OX)_{3-n}][Me_2SiO_{i/2}(OX)_{2-i}]_y$ **[1(T^n)(D^i)$_{1.5}$]** {F = $(Ph)P(CH_2CH_2OMe)(CH_2)_3-$ (**1**); $T^{n,m}$, D^i: T type (three oxygen neighbors) and D type (two oxygen neighbors) silicon atom; i, m, n = number of Si–O–Si bonds}, and the polymeric (ether–phosphine)ruthenium(II) complexes $[F-SiO_{n/2}(OX)_{3-n}]_3[MeSiO_{m/2}(OX)_{3-m}]_y$ **[2(T^n)$_3$(T^m)$_y$]** and $[F-SiO_{n/2}(OX)_{3-n}]_3[Me_2SiO_{i/2}(OX)_{2-i}]_{4.6}$ **[2(T^n)$_3$(D^i)$_{4.6}$]** {F = $[HRuCl(CO)]_{1/3}(Ph)P(CH_2CH_2OMe)(CH_2)_3-$ (**2**); y = 0, 6, 12, 18, 24, 48, 96}. These materials have been formed from the corresponding monomers (vide supra) $F-Si(OMe)_3$ **1(T^0)** and **2(T^0)$_3$**, respectively {F = $(Ph)P(CH_2CH_2OMe)(CH_2)_3-$ (**1**), $[HRuCl(CO)]_{1/3}(Ph)P(CH_2CH_2OMe)(CH_2)_3-$ (**2**)} (Schemes 1 and 2, Table 1). In contrast, the polysiloxane-bound ruthenium complex **2(T^n)$_3$(T$^m_{PMS}$)$_y$** (PMS = polymethylsiloxane) has been obtained according to method 2 from the polymer[13] $[F-SiO_{n/2}(OX)_{3-n}]_3$ **[2(T^n)$_3$]** {F = $[HRuCl(CO)]_{1/3}(Ph)P(CH_2CH_2OMe)(CH_2)_3$ – (**2**)}.

---

(10) Dorsey, J. G.; Dill, K. A. *Chem. Rev.* **1989**, *59*, 331.
(11) Dill, K. A. *J. Phys. Chem.* **1987**, *91*, 1980.
(12) Marquse, J. A.; Dill, K. A. *J. Chem. Phys.* **1986**, *85*, 434.
(13) Lindner, E.; Kemmler, M.; Mayer, H. A. *Chem. Ber.* **1992**, *125*, 2385.

Scheme 2[a]

Idealized Polycondensation

$$\underset{\mathbf{1(T^0),\ 2(T^0)_3}}{\mathrm{F{-}Si(OMe)_3}} + \mathrm{y}\ \underset{\mathbf{T^0}}{\mathrm{MeSi(OMe)_3}} \xrightarrow[-3(1+y)\mathrm{MeOH}]{\frac{3(1+y)}{2}\mathrm{H_2O}} \underset{\mathbf{1(T^3)(T^3)_y,\ 2(T^3)_3(T^3)_y}}{\mathrm{[F{-}SiO_{3/2}][MeSiO_{3/2}]_y}} \tag{1}$$

Realistic Composition of the Polycondensate: $\underset{\mathbf{1(T^n)(T^m)_y,\ 2(T^n)_3(T^m)_y}}{\mathrm{[F{-}SiO_{n/2}(OX)_{3-n}][MeSiO_{m/2}(OX)_{3-m}]_y}}$

$$\underset{\mathbf{2(T^n)_3}}{\mathrm{F{-}SiO_{n/2}(OX)_{3-n}}} + \mathrm{y}\ \underset{\mathbf{T^0}}{\mathrm{MeSi(OMe)_3}} \xrightarrow[-3\,y\,\mathrm{MeOH}]{+3\,y/2\,\mathrm{H_2O}} \underset{\mathbf{2(T^n)_3(T^m_{PMS})_y}}{\mathrm{[F{-}SiO_{n/2}(OX)_{3-n}][MeSiO_{m/2}(OX)_{3-m}]_y}} \tag{2}$$

Idealized Polycondensation

$$\underset{\substack{\mathbf{1(T^0),\ 2(T^0)_3} \\ \mathbf{3(T^0)_2}}}{\mathrm{F{-}Si(OMe)_3}} + \mathrm{y}\ \underset{\mathbf{D^0}}{\mathrm{Me_2Si(OEt)_2}} \xrightarrow[-3\mathrm{MeOH},\ -2y\,\mathrm{EtOH}]{(3/2+y)\mathrm{H_2O}} \underset{\substack{\mathbf{1(T^3)(D^2)_y,\ 2(T^3)_3(D^2)_y,} \\ \mathbf{3(T^3)_2(D^2)_y}}}{\mathrm{[F{-}SiO_{3/2}][Me_2SiO_{2/2}]_y}} \tag{3}$$

Realistic Composition of the Polycondensate: $\underset{\substack{\mathbf{1(T^n)(D^i)_y,\ 2(T^n)_3(D^i)_y,} \\ \mathbf{3(T^n)_2(D^i)_y}}}{\mathrm{[F{-}SiO_{n/2}(OX)_{3-n}][Me_2SiO_{i/2}(OX)_{2-i}]_y}}$

[a] F = (Ph)P(CH_2CH_2OMe)$CH_2CH_2CH_2$– (**1**). F = [HRuCl(CO)]$_{1/3}$P(Ph)($CH_2CH_2CH_2OMe$)$CH_2CH_2CH_2$– (**2**). F = [Cl_2Pd]$_{1/2}$P(Ph)(CH_2-CH_2OMe)$CH_2CH_2CH_2$– (**3**). $T^{n,m}$: T type silicon atom (three oxygen neighbors). D^i: D type silicon atom (two oxygen neighbors). *i*, *m*, *n* = number of Si–O–Si bonds. X = H, Me, Et. *y* = number of co-condensated T, D silicon atoms. P~O: η^1-P-coordinated ether–phosphine ligand PhP(CH_2CH_2OMe)(CH_2)$_3$Si(OMe)$_3$ and PhP(CH_2CH_2OMe)$CH_2CH_2CH_2SiO_{n/2}(OH)_{3-n}$, respectively. PMS: T-type polymethylsiloxane, prepared according to method 2, see also Experimental Section.

Table 1. Labeling of the Products of the Polycondensation Reactions

educt	co-condensation agents	amt of co-condensate	product labeling
$(MeO)_3Si(CH_2)_3(Ph)PCH_2CH_2OMe$ [$\mathbf{1(T^0)}$]	$MeSi(OMe)_3$ ($\mathbf{T^0}$)	2	$\mathbf{1(T^n)(T^m)_2}$
$(MeO)_3Si(CH_2)_3(Ph)PCH_2CH_2OMe$ [$\mathbf{1(T^0)}$]	$Me_2Si(OMe)_2$ ($\mathbf{D^0}$)	1.5	$\mathbf{1(T^n)(D^i)_{1.5}}$
HRuCl(CO)(P~O)$_3$ [$\mathbf{2(T^0)_3}$]	$MeSi(OMe)_3$ ($\mathbf{T^0}$)	0,[a] 6, 12, 18, 24, 48, 96	$\mathbf{2(T^n)_3}$, $\mathbf{2(T^n)_3(T^m)_6}$, $\mathbf{2(T^n)_3(T^m)_{12}}$, $\mathbf{2(T^n)_3(T^m)_{18}}$, $\mathbf{2(T^n)_3(T^m)_{24}}$, $\mathbf{2(T^n)_3(T^m)_{48}}$, $\mathbf{2(T^n)_3(T^m)_{96}}$
HRuCl(CO)(P~O)$_3$ [$\mathbf{2(T^n)_3}$] (condensated)	$MeSi(OMe)_3$ ($\mathbf{T^0}$)	18	$\mathbf{2(T^n)_3(T^m_{PMS})_y}$, $y = 18$
	$MeSi(OMe)_3$ ($\mathbf{T^0}$)	*y*	$\mathbf{(T^m_{PMS})_y}$
HRuCl(CO)(P~O)$_3$ [$\mathbf{2(T^0)_3}$]	$Me_2Si(OMe)_2$ ($\mathbf{D^0}$)	4.6	$\mathbf{2(T^n)_3(D^i)_{4.6}}$
Cl_2Pd(P~O)$_2$ [$\mathbf{3(T^0)_2}$]	$Me_2Si(OMe)_2$ ($\mathbf{D^0}$)	1.8, 2.4, 2.7	$\mathbf{3(T^n)_2(D^i)_{1.8}}$, $\mathbf{3(T^n)_2(D^i)_{2.4}}$, $\mathbf{3(T^n)_2(D^i)_{2.7}}$

[a] See also ref 13.

Because of the low solubility of the monomeric palladium complex F–Si(OMe)$_3$ [$\mathbf{3(T^0)_2}$] {F = (Cl_2Pd)$_{1/2}$-(Ph)P(CH_2CH_2OMe)(CH_2)$_3$– (**3**)} in methanol this starting compound was subjected to the sol–gel process as described in method 3. To maintain uniform reaction conditions for all polycondensation reactions mentioned in this paper, only Sn(OAc)$_2$(*n*-Bu)$_2$ was used as the polycondensation catalyst. Other acidic or basic catalysts like HCl, NH_4F, or NaOH lead to decomposition of some of the monomers $\mathbf{1(T^0)}$, $\mathbf{2(T^0)_3}$, and $\mathbf{3(T^0)_2}$. The total condensation of the Si–OH units (only T^3 and D^2 units; Scheme 2, Table 1) could not be achieved. We also found variable amounts of T^2, T^1, and D^1 species with two Si–O–Si bonds or one Si–O–Si bond in the synthesized polymers $\mathbf{1(T^n)(T^m)_2}$, $\mathbf{1(T^n)(D^i)_{1.5}}$, $\mathbf{2(T^n)_3(T^m)_y}$, $\mathbf{2(T^n)_3(T^m_{PMS})_y}$, $\mathbf{2(T^n)_3(D^i)_{4.6}}$, and $\mathbf{3(T^n)_2(D^i)_y}$. Further un-cross-linked –Si(OH)$_n$ and unhydrolyzed –Si(OR)$_n$ (*n* = 3, 2) groups were incorporated in the polysiloxane networks as well. As a consequence of the incomplete polycondensation an excess amount of water has to be involved in the sol–gel reaction to obtain a high degree of hydrolysis.

^{31}P, ^{13}C, ^{29}Si CP MAS NMR and IR Spectroscopic Characterization of the Polymers. The chemical shifts in the solid-state ^{31}P CP MAS NMR spectra of the polymeric ether–phosphine ligands $\mathbf{1(T^n)(T^m)_2}$ and $\mathbf{1(T^n)(D^i)_{1.5}}$, the ruthenium complexes $\mathbf{2(T^n)_3(T^m)_y}$, $\mathbf{2(T^n)_3(D^i)_{4.6}}$, and $\mathbf{2(T^n)_3(T^m_{PMS})_y}$, and the palladium complexes *cis/trans*-$\mathbf{3(T^n)_2(D^i)_y}$ are comparable to those of their monomeric congeners $\mathbf{1(T^0)}$, $\mathbf{2(T^0)_3}$,[13] and $\mathbf{3(T^0)_2}$[14] in solution (Table 2). One signal has been observed in the ^{31}P CP MAS NMR spectra of $\mathbf{1(T^n)(T^m)_2}$ and $\mathbf{1(T^n)(D^i)_{1.5}}$. The absence of other peaks indicates that phosphine oxides or other phosphine species were not formed during the polycondensation reaction.[15,16] The spectra of the co-condensated ruthenium complexes $\mathbf{2(T^n)_3(T^m)_y}$, $\mathbf{2(T^n)_3(D^i)_{4.6}}$, and $\mathbf{2(T^n)_3(T^m_{PMS})_y}$ are characterized by two isotropic signals, due to the different phosphorus nuclei P^2 and P^1 (Figure 1, Table 2, Scheme 1). The chemical shift dispersion of such materials and the occurrence of diastereomers (chirality of the ether–phosphine ligand) prevent the observation of the coupling ($^2J_{PP}$) between the two phosphorus atoms.

In the carbonyl region of the IR spectra of the ruthenium functionalized polymers only one C≡O absorption is present. Its frequency is comparable to that of the monomeric precursor $\mathbf{2(T^0)_3}$[13] in solution.

---

[14] Lindner, E.; Schreiber, R.; Kemmler, M.; Mayer, H. A.; Fawzi, R.; Steimann, M. *Z. Anorg. Allg. Chem.* **1993**, *619*, 202.

[15] Blümel, J. *GIT Fachz. Lab.* **1994**, *5*, 510.

[16] Blümel, J. *Inorg. Chem.* **1994**, *33*, 5050.

Table 2. ^{31}P CP MAS, T_{PH}, $T_{1\varrho H}$, and T_{1P} Data of the Ether−Phosphine Ligand 1 and the Polysiloxane-Bound Complexes 2 and 3

compound	^{31}P [ppm]	T_{PH}[a] [ms]	$T_{1\varrho H}$[b] [ms]	$T_{1\varrho H}$[c] [ms]	$\nu_{1/2}$ [Hz]	T_{1P}[d] [s]
$\mathbf{1(T^n)(Q^k)_2}$[e]	−32.9	0.58	2.93	2.5	642	5.2
$\mathbf{1(T^n)(T^m)_2}$	−32.8	1.54	2.0	2.2	196	
$\mathbf{1(T^n)(D^i)_{1.5}}$	−32.7	3.03	32.2	3.6	58	
$\mathbf{2(T^n)_3(Q^k)_6}$	17.3	0.21	5.83	5.5	1410	7.0
	−0.3	0.22				
$\mathbf{2(T^n)_3(T^m)_6}$	15.7	0.22	7.82	5.2	1325	
	−2.1	0.27				
$\mathbf{2(T^n)_3(D^i)_{4.6}}$	16.0	0.21	7.84	6.0	1168	
	−3.2	0.25				
$\mathbf{3(T^n)_2(D^i)_{1.8}}$	8.5	0.3	7.1	9.2	1539	
	20					
$\mathbf{3(T^n)_2(D^i)_{2.4}}$	8.4	0.3	7.3	10.2	1389	
	20.2					
$\mathbf{3(T^n)_2(D^i)_{2.7}}$	8.1	0.2	7.6	9.8	1302	
	19.8					

[a] Determined by a contact time variation. [b] Determined via ^{31}P, with the experiment according to Schaefer (see Experimental Section). [c] Measured via ^{29}Si. [d] Values from the NMR experiment of Torchia (see Experimental Section) at 297 K. [e] $\mathbf{1(T^0)}$ reacted with Si(OEt)$_4$ ($\mathbf{Q^0}$), ($k = 0-4$, number of Si−O−Si bonds); see ref 8.

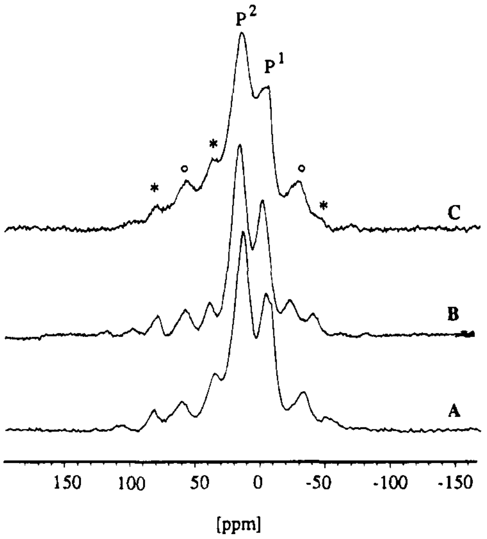

Figure 1. ^{31}P CP MAS NMR spectra of the polymer anchored complexes $\mathbf{2(T^n)_3(D^i)_{4.6}}$ (A); $\mathbf{2(T^n)_3(T^m)_6}$ (B); $\mathbf{2(T^n)_3(Q^k)_6}$ (C). The spinning side bands of P^1 and P^2 are labeled with * and O, respectively.

Each of the ^{31}P CP MAS NMR spectra of the co-condensated (ether−phosphine)palladium complexes $\mathbf{3(T^n)_2(D^i)_y}$ (y = 1.8, 2.4, 2.7) show two signals at 8 and 20 ppm, which can be assigned to *trans*- and *cis*-$\mathbf{3(T^n)_2(D^i)_y}$. Both ^{31}P signals of each compound display the same cross polarization characteristics (T_{PH} and $T_{1\varrho H}$, Table 2). The *cis:trans* ratio of $\mathbf{3(T^n)_2(D^i)_y}$ was determined to be 20:80 by integration of the ^{31}P CP MAS NMR resonances.

In addition to the ^{13}C resonances, which are attributed to the phenyl and ether carbon atoms, the ^{13}C CP MAS NMR spectra of the supported ligands $\mathbf{1(T^n)(T^m)_2}$ and $\mathbf{1(T^n)(D^i)_{1.5}}$, and of the complexes $\mathbf{2(T^n)_3(T^m)_y}$, $\mathbf{2(T^n)_3(T^m_{PMS})_y}$, $\mathbf{2(T^n)_3(D^i)_{4.6}}$, and $\mathbf{3(T^n)_2(D^i)_y}$ reveal a complex pattern in the region between 27 and 11 ppm. It comprises the ^{13}C signals of the C$_3$ spacer carbon atoms, indicating the existence of the intact carbon−phosphorus and carbon−silicon bonds,[17] and the integrity of the ligand backbone. The carbon atoms of the ligands adjacent to the ether oxygen atoms (OCH$_2$ and OMe groups) give rise to ^{13}C resonances, which are well separated from the other signals.

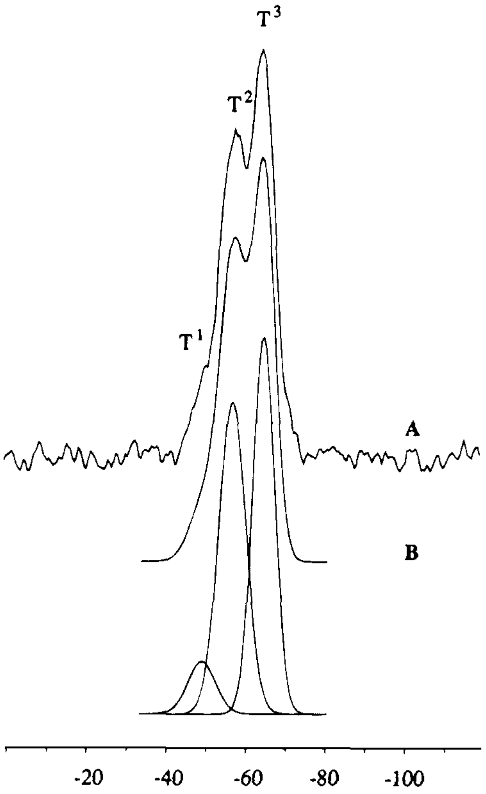

Figure 2. ^{29}Si CP MAS NMR spectrum of $\mathbf{2(T^n)_3(T^m)_6}$ (A). Peak deconvolution by simulated T^1, T^2, and T^3 resonances (B).

After the hydrolysis of the reaction mixtures MeSi(OMe)$_3$ ($\mathbf{T^0}$)/ether−phosphine ligand $\mathbf{1(T^0)}$ or MeSi(OMe)$_3$ ($\mathbf{T^0}$)/ruthenium complex $\mathbf{2(T^0)_3}$ the groups T^{n,m} were generated. It is not possible to distinguish between the different T^n and T^m units by their chemical shifts in the ^{29}Si CP MAS NMR spectra. Therefore only one group of signals has been observed, corresponding to the various substructured T species: T^1: −50 ppm, T^2: −57 ppm, T^3: −65 ppm (Figure 2).[18,19] However, if Me$_2$Si(OEt)$_2$ ($\mathbf{D^0}$) was co-condensated with $\mathbf{1(T^0)}$, $\mathbf{2(T^0)_3}$, and $\mathbf{3(T^0)_2}$ the different substructures of the T^n and D^i units were resolved: D^0: −6 ppm; D^1: −14 ppm; D^2: −22 ppm. The chemical shifts of the T^n groups remain nearly unchanged (Figure 3). To estimate the quantitative ratios of the silyl species, first the peak areas of the silicon atoms have to be determined by peak deconvolution of the ^{29}Si CP MAS NMR spectra (Figure 2). Secondly the obtained peak areas of the silyl species have to be corrected due to the different cross polarization and relaxation parameters T_{SiH} and $T_{1\varrho H}$. Subsequently a quantitative determination of the relative amount I_0 of the silyl species in the T/T and T/D blends can be drawn by the application of eq 4, using the

$$I(T_c) = \frac{I_0}{(1 - T_{SiH}/T_{1\varrho H})}(e^{-T_c/T_{1\varrho H}} - e^{-T_c/T_{SiH}}) \qquad (4)$$

boundary condition $T_{SiH} \ll T_{1\varrho H}$.[20] The essential T_{SiH}

---

(17) Corriu, R. J. P.; Moreau, J. J. E.; Thepot, P.; Wong Chi Man, M. *J. Mater. Chem.* **1994**, *4*, 987.

(18) Maciel, G. E.; Sindorf, D. W. *J. Am. Chem. Soc.* **1980**, *102*, 7606.

(19) Williams, E. A. NMR Spectroscopy of Organosilicon Compounds. In *Chemistry of Organic Silicon Compounds*; Patai, S., Rappoport, Z., Eds.; Wiley: New York, 1989.

Table 3. Relative I_0, T_{SiH}, $T_{1\varrho H}$, and T_{1Si} Data of the T Silyl Species of $\mathbf{1(T^n)(T^m)_2}$, $\mathbf{2(T^n)_3(T^m)_y}$ (y = 0, 6, 12, 18, 24, 48, and 96), and $\mathbf{2(T^n)_3(T^m_{PMS})_y}$

compound	relative I_0 data[a]			degree of condensation [%]	T_{SiH}		$T_{1\varrho H}$[b] [ms]	$T_{1\varrho H}$[c] [ms]	$T_{1\varrho H}$[d] [ms]	$\nu_{1/2}$ [Hz]	
	T^1	T^2	T^3		T^2	T^3				T^2	T^3
$\mathbf{1(T^n)(T^m)_2}$	0.32	2.85	10	91.2	*e*	*e*	2.2	2.0		211	235
$\mathbf{2(T^n)_3}$[f]	3.88	10	3.68	66.3	1.03	1.12	5.0	5.7		329	385
$\mathbf{2(T^n)_3(Q^k)_6}$[g,h]	0.94	4.79	10	84.0			5.5				
$\mathbf{2(T^n)_3(T^m)_6}$	1.86	5.95	10	81.9	1.32	1.92	5.2	7.8	6.6	266	301
$\mathbf{2(T^n)_3(T^m)_{12}}$	1.21	4.41	10	85.4	1.52	1.73	7.9	7.9	7.9	264	281
$\mathbf{2(T^n)_3(T^m)_{18}}$	0.85	3.59	10	87.8	2.11	2.84	8.8	9.2	9.2	252	260
$\mathbf{2(T^n)_3(T^m)_{24}}$	0.64	3.71	10	88.4	2.43	3.22	10.5	11.4	10.4	248	256
$\mathbf{2(T^n)_3(T^m)_{48}}$	0.44	3.95	10	88.8	2.11	3.32	13.4	13.4	14.4	242	260
$\mathbf{2(T^n)_3(T^m)_{96}}$	0.38	3.54	10	89.4	2.63	3.29	*i*	14.4		242	252
$\mathbf{2(T^n)_3(T^m_{PMS})_y}$[k]	0.23	3.99	10	89.6	1.88	3.83	41.8	7.0		247	246
$\mathbf{(T^m_{PMS})_y}$[l]	0.22	3.72	10	90.0	3.61	3.93	41.8			247	244

[a] Calculated from eq 1. [b] Measured via ^{29}Si (T_c = 4 ms). [c] Measured via ^{31}P (T_c = 2 ms). [d] Calculated from eq 8. [e] $T_{SiH} \approx T_{1\varrho H}$; a precise determination of T_{SiH} is therefore impossible. [f] See ref 13. [g] $\mathbf{2(T^0)_3}$ reacted with $Si(OEt)_4$ ($\mathbf{Q^0}$) (k = 0−4, number of Si−O−Si bonds); see ref 8. [h] Relative I_0 data: Q^2 2.3, Q^3 10, Q^4 8.3; degree of condensation: 83%. [i] Two components of $T_{1\varrho H}$ [13.4 ms and 42.4 ms]. [k] Prepared with method 2. [l] Polymethylsiloxane.

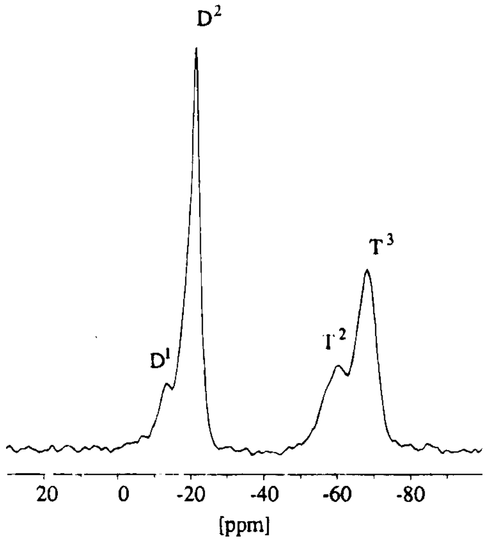

Figure 3. ^{29}Si CP MAS NMR spectrum of $\mathbf{3(T^n)_2(D^i)_{2.7}}$.

data were obtained by contact time studies of each sample (Table 3) and the $T_{1\varrho H}$ values by the pulse sequence according to Schaefer.[21]

The relative amounts of I_0 of the T^1, T^2, and T^3 groups enable one to calculate the degree of condensation (Table 3).[22]

The noncomplexed ether−phosphine ligand $\mathbf{1(T^n)(T^m)_2}$ shows the highest degree of condensation (91%). The lowest degree of condensation (66%) in the series of the ruthenium complexes $\mathbf{2(T^n)_3(T^m)_y}$ (y = 0, 6, 12, 18, 24, 48, 96) was found for $\mathbf{2(T^n)_3}$ without any co-condensate (y = 0).[8] The higher the molar amount of the added co-condensate (y), the higher is the degree of condensation in the series of the polymeric ruthenium complexes $\mathbf{2(T^n)_3(T^m)_y}$ (y = 0−96). The values show a continuous increase from 82 to 89%. The bulky complex obviously prevents a complete condensation of the hydroxyl groups.

Moreover the quantification of the silicon groups allowed the determination of the ratio T:D in the T/D blends $\mathbf{1(T^n)(D^i)_{1.5}}$, $\mathbf{2(T^n)_3(D^i)_{4.6}}$, and $\mathbf{3(T^n)_2(D^i)_y}$. Thus an adaptation of the stoichiometry of the resulting gels was possible. Although a high molar ratio between the co-condensate $Me_2Si(OEt)_2$ ($\mathbf{D^0}$) and the monomeric species $\mathbf{1(T^0)}$ and $\mathbf{2(T^0)_3}$ was employed in the polycondensation reaction of the free ether−phosphine ligand $\mathbf{1(T^n)(D^i)_y}$ and the ruthenium complex $\mathbf{2(T^n)_3(D^i)_y}$ the T:D ratio was determined to be 1.5 (y = 1.5 and 4.6, respectively). This indicates, that a substantial part of oligomeric $\mathbf{D^i}$ groups was washed out during the solvent processing. An analogous situation has been found in the case of the polycondensation of $Me_2Si(OEt)_2$ ($\mathbf{D^0}$) with *cis*/*trans*-$Cl_2Pd(P{\sim}O)_2$ [$\mathbf{3(T^0)_2}$]. The T:D ratios of the polymeric palladium complexes $\mathbf{3(T^n)_2(D^i)_y}$ were ascertained to be 1:0.9, 1:1.2, and 1:1.4, the upper limit seems to be 1:1.5. Thus the metal complex density within the T/D polymer is not controllable, in contrast to the T/T and T/Q polysiloxanes.[23] Simple $\mathbf{D^0}$ units are therefore unsuitable for building blocks of metal functionalized stationary phases. Further investigations on the applicability of other D units [for example the bifunctional precursor $(OR')_2(R')Si(CH_2)_xSi(R')(OR')_2$, R' = Me] are in progress.

Studies on the Dynamic Behavior of the Polymeric Ligands and Complexes. The line widths of the ^{31}P CP MAS NMR signals of the polymer supported ligands (Schemes 1 and 2) increase in the order $\mathbf{1(T^n)(D^i)_{1.5}}$, $\mathbf{1(T^n)(T^m)_2}$ from 58 to 128 Hz. Compared to these results $\mathbf{1(T^n)(Q^k)_2}$, a previously published[8] co-condensate of the ether−phosphine $\mathbf{1(T^0)}$ with $Si(OEt)_4$ ($\mathbf{Q^0}$) [Q type (four oxygen neighbors) silicon atom, k = 0−4, number of silicon neighbors], revealed a further increase of the line width to 640 Hz (Table 2, Figure 4). Simultaneously the T_{PH} value decreases (Table 2) in the polymeric ligand series $\mathbf{1(T^n)(D^i)_{1.5}}$ to $\mathbf{1(T^n)(Q^k)_2}$, representing a faster magnetization transfer from the protons to the phosphorus nuclei of the polymerized ligand $\mathbf{1(T^n)(Q^k)_y}$ compared to the ^{31}P nuclei of the analogous co-condensated ether−phosphine ligands $\mathbf{1(T^n)(T^m)_2}$ and $\mathbf{1(T^n)(D^i)_{1.5}}$. The long T_{PH} time of the noncoordinated ligand $\mathbf{1(T^n)(D^i)_{1.5}}$ and the low line width of its ^{31}P CP MAS NMR signal are caused by a high mobility of the phosphorus atom of $\mathbf{1(T^n)(D^i)_{1.5}}$ in the kilohertz region.[24-29]

---

(20) Harris, R. K. *Analyst* **1985**, *110*, 649.

(21) Schaefer, J.; Stejskal, E. O.; Buchdahl, R. *Macromolecules* **1977**, *10*, 384.

(22) The degree of condensation of the T species: $100(T^1 + 2T^2 + 3T^3)/[3(T^1 + T^2 + T^3)]$, degree of condensation of the D species: $100(D^1 + 2D^2)/[2(D^1 + D^2)]$.

(23) Lindner, E.; Kemmler, M.; Mayer, H. A. *Git Fachz. Lab.* **1994**, *4*, 353.

(24) Schmid-Betschinger, J. Ph.D. Dissertation, Universität Tübingen, 1989.

(25) Veemann, W. S.; Menger, E. M.; Ritchey, W.; de Boer, E. *Macromolecules* **1979**, *12*, 924.

Table 4. Relative I_0, T_{SiH}, $T_{1\varrho\mathrm{H}}$, and $T_{1\mathrm{Si}}$ Values of the Various Silyl Species in the T/D Copolymers $\mathbf{1(T^{n})(D^{i})_{1.5}}$, $\mathbf{2(T^{n})_3(D^{i})_{4.6}}$, and $\mathbf{3(T^{n})_2(D^{i})_{y}}$ (y = 1.8, 2.4, 2.7)

	relative I_0 data[a]					degree of condensation		real T/D moiety	T_{SiH} [ms][b]				$T_{1\varrho\mathrm{H}}$ [ms][c]	$T_{1\mathrm{Si}}$ [s][d]		
	D^2	D^1	D^0	T^3	T^2	D	T		D^2	D^1	T^3	T^2		D^2	T^3	T^2
$\mathbf{1(T^{n})(D^{i})_{1.5}}$	10.0	0.5	0.2	5.2	2.0	96	91	1:1.5	*e*	*e*	*e*	*e*	3.6	24.0	37.0	
$\mathbf{2(T^{n})_3(D^{i})_{4.6}}$	10.0	2.0	0.5	4.1	3.7	88	83	1:1.5	2.12		1.26	0.99	6.0	11.0	23.4	16.0
$\mathbf{3(T^{n})_2(D^{i})_{1.8}}$	10.0	3.7		8.5	7.3	86	85	1:0.9	1.95	1.36	1.37	1.09	9.2	22.0	50.8	38.4
$\mathbf{3(T^{n})_2(D^{i})_{2.4}}$	10.0	1.1		5.8	3.3	95	88	1:1.2	2.61	1.56	1.29	0.82	10.2			
$\mathbf{3(T^{n})_2(D^{i})_{2.7}}$	10.0	2.0		5.5	3.5	92	87	1:1.4	2.47	1.27	1.33	0.97	9.8			

[a] Calculated from eq 4. [b] From contact time variation. [c] Averaged value of the T and D groups. [d] Pulse sequence developed by Torchia; see ref 46. [e] The boundary condition $T_{\mathrm{SiH}} \ll T_{1\varrho\mathrm{H}}$ is not fulfilled.

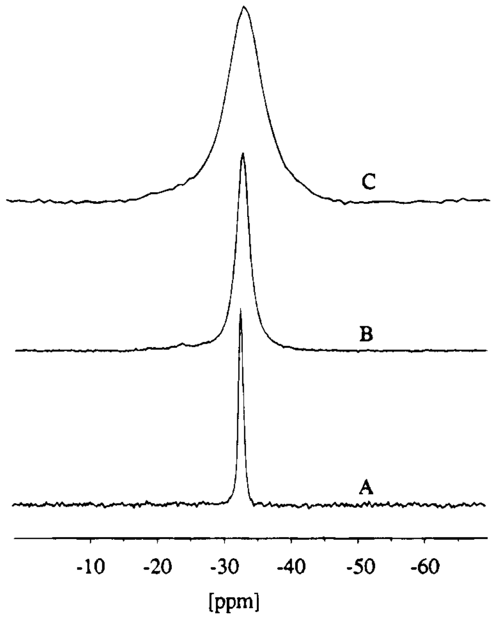

Figure 4. ^{31}P CP MAS NMR spectra of $\mathbf{1(T^{n})(D^{i})_{1.5}}$ (A), $\mathbf{1(T^{n})(T^{m})_2}$ (B), and $\mathbf{1(T^{n})(Q^{k})_2}$ (C) at 297 K, ν = 3600 Hz. Effect of the different types of co-condensates on the half line width.

In the case of the complexes $\mathbf{2(T^{n})_3(D^{i})_{4.6}}$, $\mathbf{3(T^{n})_2(D^{i})_{y}}$, and $\mathbf{2(T^{n})_3(T^{m})_{y}}$ (Scheme 1), in which the ether–phosphines $\mathbf{1(T^{n})(T^{m})_2}$ and $\mathbf{1(T^{n})(D^{i})_{1.5}}$ are coordinated to a transition-metal center, the T_{PH} values drop close to 0.3 ms (Table 2). Thus the coordination of the phosphorus donor to the metal center enables a fast polarization transfer from the protons of the *ligand backbone* to the ^{31}P nucleus for each type of co-condensate. This is caused by the lower ^{31}P flexibility of the phosphorus atom of the coordinated ligand.

The assumption of the high ^{31}P mobility of the ligand $\mathbf{1(T^{n})(D^{i})_{1.5}}$ is supported by $T_{1\varrho\mathrm{H}}$ relaxation time measurements, detected via ^{31}P solid-state NMR spectroscopy (Table 2). The difference in the $T_{1\varrho\mathrm{H}}$ relaxation times between the two T/Q and T/T blends $\mathbf{1(T^{n})(Q^{k})_2}$ and $\mathbf{1(T^{n})(T^{m})_2}$ is not significant, but $T_{1\varrho\mathrm{H}}$ increases remarkably in the case of the noncoordinated ligand $\mathbf{1(T^{n})(D^{i})_{1.5}}$ (Table 2). All three values of the relaxation times $T_{1\varrho\mathrm{H}}$ at 297 K of these polymeric ether–phosphines are located on the left side of the correlation time scale.[30] Spin diffusion is an inefficient relaxation mechanism at this side of the correlation time curve. Thus longer $T_{1\varrho\mathrm{H}}$ times correspond to higher mobilities (in the kilohertz region). Therefore the graduation of the relaxation parameter $T_{1\varrho\mathrm{H}}$ in the sequence $\mathbf{1(T^{n})(D^{i})_{1.5}} \gg \mathbf{1(T^{n})(T^{m})_2} \sim \mathbf{1(T^{n})(Q^{k})_2}$ again points to the highest mobility of the phosphorus atom in $\mathbf{1(T^{n})(D^{i})_{1.5}}$, whereas the polysiloxane-bound ligands $\mathbf{1(T^{n})(T^{m})_2}$ and $\mathbf{1(T^{n})(Q^{k})_2}$ are more rigid.

The silicon-29 solid-state NMR spectra of the ether–phosphine ligand $\mathbf{1(T^{n})(D^{i})_{1.5}}$, as well as those of the ruthenium and palladium complexes $\mathbf{2(T^{n})_3(D^{i})_{4.6}}$ and $\mathbf{3(T^{n})_2(D^{i})_{y}}$ (Scheme 2) confirm that the protons of the D methyl groups cross polarize the other NMR active nuclei (Si, P) inefficiently (fast methyl group rotation; large spatial distance to the ^{31}P nucleus).[31,32] The cross polarization times T_{SiH} (Table 4) increase in the order $T^2 < T^3 \sim D^1 < D^2$. The obtained values indicate that the matrix becomes more flexible if D^i components are incorporated in the network.[8] Marginal differences of the T_{SiH} data of the free ligand $\mathbf{1(T^{n})(D^{i})_{1.5}}$ and of the coordinated ligand [in the metal complexes $\mathbf{2(T^{n})_3(D^{i})_{4.6}}$ and $\mathbf{3(T^{n})_2(D^{i})_{y}}$ (Scheme 1)] were detected (Table 4). Thus T_{SiH} is independent of the coordination geometry of the phosphorus atom in contrast to the T_{PH} value. The flexibility of the phosphorus atoms (and therefore the cross polarization constant T_{PH}) is more affected by their coordination to the metal than the mobility of the silicon atoms.

The loss of the proton magnetization in the rotating frame ($T_{1\varrho\mathrm{H}}$) was also investigated by ^{29}Si CP MAS NMR spectroscopy. The amplitudes of the silicon resonances of the T/D polymers $\mathbf{1(T^{n})(D^{i})_{1.5}}$, $\mathbf{2(T^{n})_3(D^{i})_{4.6}}$, and $\mathbf{3(T^{n})_2(D^{i})_{y}}$ decay monoexponentially. The T and D silicon substructures within a polymer show the same $T_{1\varrho\mathrm{H}}$ relaxation times (Figure 5), indicating a strong dipole–dipole interaction between the silicon atoms and the protons and among the protons themselves (spin diffusion),[33,34] which prevents separate $T_{1\varrho\mathrm{H}}$ data for the different silicon substructures. Therefore it is not allowed to draw conclusions from the $T_{1\varrho\mathrm{H}}$ values (via ^{29}Si) on the mobility of the silicon matrixes.

However, the methyl groups of the D units contribute to the spin–lattice relaxation time $T_{1\mathrm{Si}}$. The silicon atom of each D unit of $\mathbf{1(T^{n})(D^{i})_{1.5}}$, $\mathbf{2(T^{n})_3(D^{i})_{4.6}}$, and $\mathbf{3(T^{n})_2(D^{i})_{y}}$ (Scheme 1) is characterized by shorter $T_{1\mathrm{Si}}$ values than the T^n unit in the same compound (Table 4). It is clearly recognizable that the rotating Si–CH$_3$ groups cause the relaxation ($T_{1\mathrm{Si}}$) of the silicon atoms in the megahertz region as was to be expected.[31,32]

The line widths of the ^{31}P CP MAS NMR signals of the polysiloxane supported palladium complexes $\mathbf{3(T^{n})_2}$-

---

(26) Sullivan, M. J.; Maciel, G. E. *Anal. Chem.* **1982**, *54*, 1606.

(27) Earl, W. L.; VanderHart, D. L. *Macromolecules* **1979**, *12*, 762.

(28) Myhre, P. C.; Yannoni, C. S. *J. Am. Chem. Soc.* **1981**, *103*, 230.

(29) Fyfe, C. A.; Lyerla, J. R.; Volksen, W.; Yannoni, C. S. *Macromolecules* **1979**, *12*, 757.

(30) Kemmler, M. Ph.D. Dissertation, Universität Tübingen 1994.

(31) Alemany, L. B.; Grant, D. M.; Pugmire, R. J.; Alger, T. D.; Zilm, K. W. *J. Am. Chem. Soc.* **1983**, *105*, 2133.

(32) Alemany, L. B.; Grant, D. M.; Pugmire, R. J.; Alger, T. D.; Zilm, K. W. *J. Am. Chem. Soc.* **1983**, *105*, 2143.

(33) Douglass, D. C.; McBrierty, V. J. *J. Chem. Phys.* **1971**, *54*, 4085.

(34) Assink, R. A.; Wilkes, G. C. *J. Polym. Eng. Sci.* **1977**, *17*, 606.

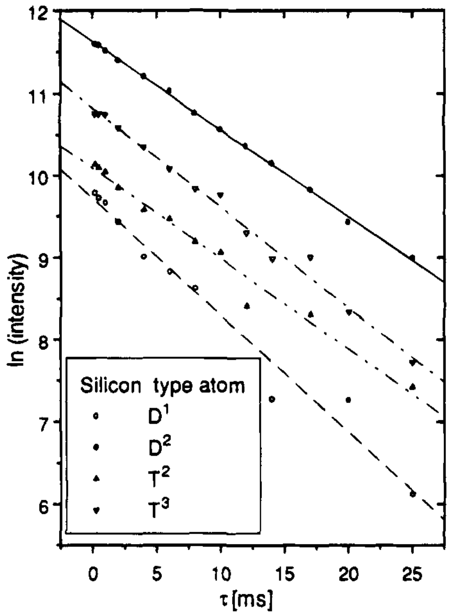

Figure 5. $T_{1\varrho H}$ of $\mathbf{3(T^n)_2(D^i)_{2.7}}$ detected by ^{29}Si CP MAS NMR spectroscopy at a contact time T_c of 10 ms.

$\mathbf{(D^i)_y}$ rise with decreasing y (Table 2). The half line widths of the ^{31}P resonances of the ruthenium complexes $\mathbf{2(T^n)_3(D^i)_{4.6}}$, $\mathbf{2(T^n)_3(T^m)_6}$, and $\mathbf{2(T^n)_3(Q^k)_6}$ [a copolymer[8] of $\mathbf{2(T^0)_3}$ with Si(OEt)$_4$ ($\mathbf{Q^0}$)] show also a tendency to this line broadening (Figure 1). This is comparable to the increase of the line width of the polymer anchored ligands $\mathbf{1(T^n)(D^i)_{1.5}}$, $\mathbf{1(T^n)(T^m)_2}$, and $\mathbf{1(T^n)(Q^k)_2}$ (Figure 4).

In the series of the ruthenium complexes $\mathbf{2(T^n)_3(D^i)_{4.6}}$, $\mathbf{2(T^n)_3(T^m)_6}$, and $\mathbf{2(T^n)_3(Q^k)_6}$ and in contrast to the series of the corresponding ligands $\mathbf{1(T^n)(D^i)_{1.5}}$, $\mathbf{1(T^n)(T^m)_2}$, and $\mathbf{1(T^n)(Q^k)_2}$ neither the relaxation times $T_{1\varrho H}$ (via ^{31}P) nor the cross-polarization constants T_{PH} differ considerably (Table 2). As mentioned above, the parameter T_{PH} of the phosphorus nuclei of all ruthenium and palladium complexes are on the same low level (fast magnetization transfer) and thus do not depend on the kind of the co-condensate. The relaxation times in the rotating frame $T_{1\varrho H}$ (detected via ^{31}P) of the coordinated ether–phosphines $\mathbf{2(T^n)_3(D^i)_{4.6}}$, $\mathbf{2(T^n)_3(T^m)_6}$, $\mathbf{2(T^n)_3(Q^k)_6}$, and $\mathbf{3(T^n)_2(D^i)_y}$ are in the same range. These values do not vary with different contact times during the pulse sequence of Schaefer.[21] No difference of the rigidity of the polymer anchored ruthenium and palladium complexes can be deduced from the NMR data, because either their T_{PH}'s or their $T_{1\varrho H}$'s (via ^{31}P and ^{29}Si) are comparable. We assume that different glass transition temperatures T_g[35] may be responsible for the different ^{31}P resonance line widths of the above-mentioned polymer-supported complexes $\mathbf{2(T^n)_3(D^i)_{4.6}}$, $\mathbf{2(T^n)_3(T^m)_6}$, $\mathbf{2(T^n)_3(Q^k)_6}$, and $\mathbf{3(T^n)_2(D^i)_y}$ (Scheme 2).

Domains in transition-metal-functionalized stationary T/Q phases were found to have a strong influence on the catalytic behavior of the supported complex. This segregation takes place if a higher amount of the Q co-condensate is used during the polycondensation reaction.[8] Therefore we were also interested, whether T/T blends of the complexes show a tendency to build up domains with their co-condensates.

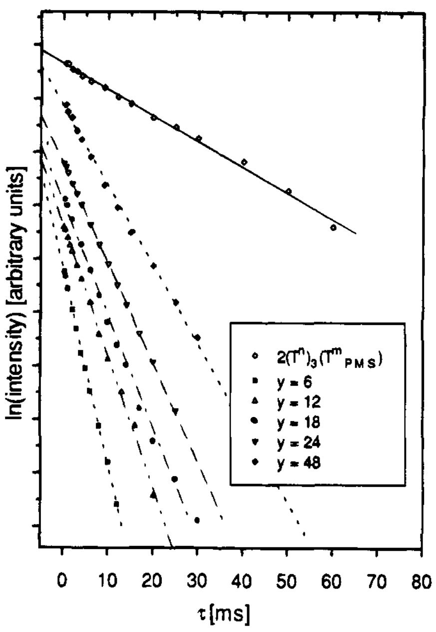

Figure 6. Effect of increasing amount of co-condensate on $T_{1\varrho H}$ via ^{29}Si: T^3 units of $\mathbf{2(T^n)_3(T^m)_y}$ and $\mathbf{2(T^n)_3(T^m_{PMS})_y}$.

A simple way to form such domains is the reaction of the polymeric ruthenium complex $\mathbf{2(T^n)_3}$ with monomeric MeSi(OMe)$_3$ ($\mathbf{T^0}$) units (according to method 2, Scheme 2). The resulting gel should be composed of $\mathbf{2(T^n)_3}$ blocks caged by $\mathbf{T^m_{PMS}}$ silicon units. The spectroscopic data of this inhomogeneous matrix $\mathbf{2(T^n)_3(T^m_{PMS})_y}$ (vide supra) can be compared to those of the stationary phases $\mathbf{2(T^n)_3(T^m)_y}$, which were formed from homogeneous mixtures with different amounts of the co-condensate (method 1).

A series of polymer anchored (ether–phosphine)-ruthenium complexes $\mathbf{2(T^n)_3(T^m)_y}$ (y = 0–96, Scheme 2) was synthesized. The line widths in the ^{29}Si CP MAS NMR spectra in this series have been reduced by 26% (T^2) and 35% (T^3), respectively. The line narrowing is accompanied by a continuous increase of the cross polarization time T_{SiH} (Table 3). The T_{SiH} value of the T^2-type silicon atoms is shorter than that of the T^3 group. Both sets of data point to an increasing flexibility of the polysiloxane network with increasing y.

The siloxane caged ruthenium complex $\mathbf{2(T^n)_3(T^m_{PMS})_y}$ shows a very long T_{SiH} value of the T^3 unit and a T_{SiH} value of the T^2 group, which is located between the two extreme data of $\mathbf{2(T^n)_3}$ and $\mathbf{2(T^n)_3(T^m)_{96}}$. Finally pure polymethylsiloxane ($\mathbf{T^m_{PMS}}$)$_y$ reveals T_{SiH} data of the T^2 and T^3 substructures, representing the upper levels of all measured values in this series.

The $T_{1\varrho H}$ values (via ^{31}P or via ^{29}Si) of the copolymerized ruthenium complexes $\mathbf{2(T^n)_3(T^m)_y}$ are also depending on the number y of the added co-condensate $\mathbf{T^0}$ (Table 3). Longer $T_{1\varrho H}$ values have been measured for higher amounts of the co-condensate (Figure 6). The loss of the proton magnetization in the rotating frame, detected via ^{29}Si, is monoexponential for y = 0–48. A biexponential decay of the proton magnetization has been observed for y = 96 (Table 3), indicating the formation of aggregates with different molecular composition.

The $T_{1\varrho H}$ data obtained by the ^{31}P CP MAS NMR spectra as well as those by the ^{29}Si CP MAS NMR spectra are in the same scale (within the limit of error). However, in the case of the ruthenium complex $\mathbf{2(T^n)_3}$-

---

[35] Komoroski, R. A. *High Resolution NMR Spectroscopy of Synthetic Polymers in Bulk*; VCH Publishers, Inc.: Deerfield Beach, FL, 1986; pp 63, 247.

$(\mathbf{T}^m_{\mathbf{PMS}})_y$ there is a big difference between the relaxation times $T_{1\varrho H}$ detected via ^{31}P or via ^{29}Si. A value close to that of the polymer $\mathbf{2(T}^n\mathbf{)_3}$ has been observed (7 ms) with phosphorus as the probe for the proton magnetization, whereas with silicon 29 the high value of the polymethylsiloxane matrix $(\mathbf{T}^m_{\mathbf{PMS}})_y$ has been measured (41.8 ms). This indicates that $\mathbf{2(T}^n\mathbf{)_3(T}^m_{\mathbf{PMS}}\mathbf{)}_y$ is set up by $\mathbf{2}$-$\mathbf{(T}^n\mathbf{)_3}$ particles caged by $\mathbf{T}^m_{\mathbf{PMS}}$ units. A two-phase system is derived from these data for the compound $\mathbf{2(T}^n\mathbf{)_3(T}^m_{\mathbf{PMS}}\mathbf{)}_y$.

Spin diffusion among the protons leads to uniform $T_{1\varrho H}$'s (via ^{31}P or ^{29}Si) for $y = 0-48$, but for $y = 96$ the interaction between the protons of the ruthenium complex $\mathbf{2(T}^n\mathbf{)_3(T}^m\mathbf{)_{96}}$ and the hydrogen atoms located in the matrix is interrupted,[36] which causes different $T_{1\varrho H}$'s via ^{31}P and ^{29}Si. This result renders it possible to estimate the distance L over which spin diffusion is maintained. Equation 5 relates the distance L with the available time of the spin diffusion[37] of the siloxane-bound ruthenium complex $\mathbf{2(T}^n\mathbf{)_3(T}^m\mathbf{)_{48}}$.

$$L = l_0\sqrt{T_{1\varrho H}/T_2} \tag{5}$$

For $l_0 = 0.1$ nm [(distance between two protons), $T_{1\varrho H} = 13.4$ ms (Table 3) and $T_2 = 15$ μs] the observed diameter for spin diffusion is calculated to be $L = 3$ nm. Therefore, if segregation of the matrix components is present, the linear dimensions of these aggregates are less than 3 nm on the basis of the $T_{1\varrho H}$ data. VanderHart[38,39] has proposed that the distance L, over which ^{1}H spin diffusion occurs during a time t can be expressed by eq 6 (with $t = T_{1\varrho H} = k^{-1}$) from which a value of $D =$

$$L = \sqrt{6D/k} \tag{6}$$

10^{-12} cm^2/s is calculated, a typical result for the spin diffusion coefficient of organic polymers.[39-42] The relaxation rate is related to the number N_1 (55), N_2 ($3y$) of the protons of the two components $\mathbf{2(T}^n\mathbf{)_3}$ and $(\mathbf{T}^m_{\mathbf{PMS}})_y$ by eq 7[37,39,43-45] where k_c is the calculated or

$$k_c = k_1\frac{N_1}{N_1 + N_2} + k_2\frac{N_2}{N_1 + N_2} \tag{7}$$

the observed rotating frame relaxation rate ($T_{1\varrho H}{}^{-1}$) of the stationary phase, k_1, k_2 are the relaxation rates of the two components $\mathbf{2(T}^n\mathbf{)_3}$ and $(\mathbf{T}^m_{\mathbf{PMS}})_y$ (1/5 and 1/41.5 ms^{-1}, Table 3) in the polymer. Equation 7 may be written in terms of the molar amount y of the co-condensate T^0:

$$k_c(55 + 3y) = 55k_1 + 3yk_2 \tag{8}$$

The experimental relaxation rates (k_{obs}) are in good agreement with the $T_{1\varrho H}{}^{-1}$ values (k_{calc}) calculated from eq 8 (Table 3, Figure 7). The linear plot indicates molecularly compatible blends for $y = 0-48$. With the experimental data of D, we received for $\mathbf{2(T}^n\mathbf{)_3(T}^m\mathbf{)_6}$ (with its shorter $T_{1\varrho H}$) a spin diffusion distance of $L = 1.8$ nm, which is in the range of the diameter of the ruthenium complex HRuCl(CO)(P~O)$_3$ $[\mathbf{2(T}^0\mathbf{)_3}]$.

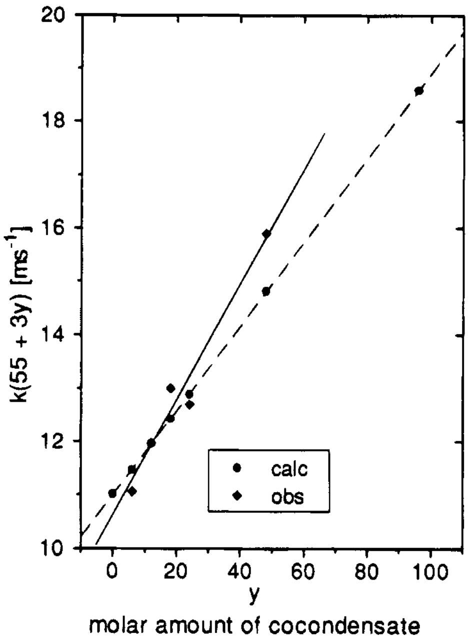

Figure 7. Plot of $(55 + 3y)k$ vs y, the amount of the co-condensate. Composition dependence on the relaxivity of $\mathbf{2(T}^n\mathbf{)_3(T}^m\mathbf{)}_y$ blends. The dash line is calculated from eq 8.

In the polysiloxane-bound complex $\mathbf{2(T}^n\mathbf{)_3(T}^m\mathbf{)_{96}}$, in which the spin diffusion process is interrupted, we assume that the distances between the aggregates containing the complexes with a 2(T^n)$_3$ unit and of the polymethylsiloxane-like components (T^m) are larger than 3 nm. The available data demonstrate that these organic–inorganic siloxane networks can be handled like blends of several organic polymers.

Conclusion

Polysiloxane-bound (ether–phosphine)palladium(II) and ruthenium(II) complexes belonging to a new class of polymer-supported catalysts have been prepared by hydrolysis and polycondensation of silyl-functionalized metal complexes with several D- and T-types of alkoxysilanes. ^{29}Si and ^{31}P solid-state NMR spectroscopy were employed to investigate the flexibility and the distribution of the material components. The $T_{1\varrho H}$ and T_{SiH} data of the D-modified polymers indicate much higher mobilities of the supported ligands and the matrix elements than of the T- or Q-modified species. These attributes of the polymers, which are built up by D units, are supposed to be appropriate in catalytic reactions but the high solubilities make them unsuitable for use in interphase reactions. The composites metal complex/co-condensate (D, T) reveal no tendency to aggregation or unmixing of one of the components, which was studied by solid-state NMR spectroscopy. At high amounts of co-condensated (T-) matrix components we found areas with properties of a metal complex–co-condensate mixture and areas with the features of pure poly(methylsiloxane), respectively. Also from this point of view materials with D- or T-type silicon functions as the co-condensation agent represent the more favorable catalysts than those with Q-type silicon atoms. Therefore, currently we are investigating the properties of polysiloxane-bound complexes formed from bisilylated

---

[36] Voelkel, R. *Angew. Chem., Int. Ed. Engl.* **1988**, *27*, 1468.

[37] Dickinson, L. C.; Yang, H.; Chu, C.-W.; Stein, R. S.; Chien, J. C. W. *Macromolecules* **1987**, *20*, 1757.

[38] Havens, J. R.; VanderHart, D. L. *Macromolecules* **1985**, *18*, 1663.

[39] Yang, H.; Kwei, T. K.; Dai, Y. *Macromolecules* **1993**, *20*, 842.

[40] Assink, R. A. *Macromolecules* **1978**, *11*, 1233.

[41] VanderHart, D. L. *Makromol. Chem., Macromol. Sym.* **1990**, *34*, 125.

[42] Douglass, D. C.; Jones, G. P. *J. Chem. Phys.* **1965**, *45*, 956.

D-functionalized matrix component precursors, which could lead to a more favorable solubility and swelling.

Experimental Section

The elemental analyses were carried out on a Carlo Erba analyzer, Model 1106. IR data were obtained on a Bruker IFS 48 FT-IR spectrometer. The CP MAS solid-state NMR spectra were recorded on a Bruker MSL 200 multinuclear spectrometer with a wide bore magnet (4.7 T). All measurements were carried out under exclusion of molecular oxygen. Frequencies and standards: ^{31}P, 81 MHz ($NH_4H_2PO_4$); ^{13}C, 50.325 MHz [TMS, carbonyl resonance of glycin ($\delta = 170.09$) as the second standard]; ^{29}Si, 39.75 MHz (Q_8M_8). The cross-polarization constants T_{PH} and T_{SiH} were determined by variations of the contact time (20–25 experiments). The proton relaxation time in the rotating frame $T_{1\varrho H}$ was measured by direct proton spin lock–τ–CP experiments as described by Schaefer and Stejskal.[21] T_{1P} and T_{1Si} values were received using the method developed by Torchia.[46] All the relaxation time data were obtained by using the Bruker software SIMFIT. Three times the highest T_{SiH} value has been used as a typical contact time T_c for the quantitative determination of the relative amount of the silyl species with eq 4. Peak deconvolution of the spectra were performed with the Bruker software GLINFIT using Gaussian line shapes. For a more detailed description of other NMR parameters see ref 8.

All manipulations were performed under argon by employing the usual Schlenk techniques. Methanol was dried with magnesium and distilled, ethanol was distilled from NaOEt. *n*-Hexane and toluene were distilled from sodium benzophenone ketyl. H_2O, $MeSi(OMe)_3$ ($\mathbf{T^0}$, Aldrich), and $Me_2Si(OEt)_2$ ($\mathbf{D^0}$, Aldrich) were distilled under inert gas prior to use. All solvents were stored under argon. The monomeric ether–phosphine $\mathbf{1(T^0)}$[8,9] and the starting complexes $\mathbf{2(T^0)_3}$,[13] and $\mathbf{3(T^0)_2}$[14] were synthesized as described previously.

Sol–Gel Processing. Method 1. $\mathbf{1(T^n)(T^m)_2}$, $\mathbf{2(T^n)_3(T^m)_y}$ ($\mathbf{y}$ = 6, 12, 18, 24, 48, 96) and $\mathbf{(T^m_{PMS})_y}$. The ether–phosphine $(Ph)P(CH_2CH_2OMe)(CH_2)_3Si(OMe)_3$ [$\mathbf{1(T^0)}$] or $HRuCl(CO)(P{\sim}O)_3$ [$\mathbf{2(T^0)_3}$] was dispersed in a mixture of $(n\text{-}Bu)_2Sn(OAc)_2$, the specified quantity of water, and $MeSi(OMe)_3$ ($\mathbf{T^0}$) and was stirred vigorously in a sealed Schlenk tube at room temperature. A few minutes later the heterogeneous mixture became homogeneous, due to the elimination of methanol during the hydrolysis. After this was stirred for 60 min at room temperature, the solvent was removed under vacuum. The polymers were placed on a paper filter, washed with 200 mL of acetone and *n*-hexane, and dried under vacuum. Further stirring in *n*-hexane overnight produced fine powders, which were dried under vacuum at 60 °C for 4 h. After solvent processing and aging white powders of $\mathbf{1(T^n)(T^m)_2}$, or $\mathbf{(T^m_{PMS})_y}$, or a creamy-white powder of $\mathbf{2(T^n)_3(T^m)_y}$ were formed.

(2-Methoxyethyl)phenyl(polysiloxanylpropyl)phosphine $\mathbf{(T^m)_2}$ [$\mathbf{1(T^n)(T^m)_2}$]. A mixture of the O,P ligand $\mathbf{1(T^0)}$ (380 mg, 1.152 mmol), 2 equiv of $MeSi(OMe)_3$ ($\mathbf{T^0}$ 313 mg, 2.3 mmol), water (120 mg, 6.21 mmol), and $(n\text{-}Bu)_2Sn(OAc)_2$ (13 mg, 0.038 mmol) was sol–gel processed to give a colorless gel. After solvent processing and aging a white powder was formed. [$\mathbf{1(T^n)(T^m)_2}$, 420 mg, 92%]: ^{29}Si CP MAS NMR (silicon substructure) δ −51.2 (T^1), −57.7 (T^2), −65.8 (T^3); IR (KBr) 3429, 3071, 2929, 1436, 1273, 1114, 1027, 778, 744, 696 cm^{-1}. Anal. Calcd for $C_{14}H_{24}O_{5.5}PSi_3$[47] (idealized stoichiometry): C, 42.51; H, 6.12. Corrected stoichiometry:[48] C, 41.76; H, 6.21. Found: C, 38.20; H, 6.29.

Carbonylchlorohydridotris[(2-methoxyethyl)phenyl(polysiloxanylpropyl)phosphine-*P,P′,P″*]ruthenium(II) $\mathbf{(T^m)_6}$ [$\mathbf{2(T^n)_3(T^m)_6}$]. A mixture of $HRuCl(CO)(P{\sim}O)_3$ [$\mathbf{2(T^0)_3}$] (438 mg, 0.379 mmol), 6 equiv of $MeSi(OMe)_3$ ($\mathbf{T^0}$ 309 mg, 2.274 mmol), water (111 mg, 6.14 mmol), and $(n\text{-}Bu)_2Sn(OAc)_2$ (13 mg, 0.038 mmol) was sol–gel processed to give a slightly yellow gel. [$\mathbf{2(T^n)_3(T^m)_6}$, 502 mg, 98%]: ^{29}Si CP MAS NMR (silicon substructure) δ −49.5 (T^1), −56.5 (T^2), −64.8 (T^3); ^{13}C CP MAS NMR (TOSS, 3.3 kHz) δ 138.0 (C-*i*), 129.0 (C-*o*, -*m*, -*p*), 69.0 (C-5), 58.1 (C-6), 51.0 ($SiOCH_3$), 27.2 (C-3, 4), 18.1 (C-2), 13.8 (C-1), −3.9 ($SiCH_3$); IR (KBr) 3412, 3057, 2935, ν(CO) 1918, 1436, 1272, 1109, 1027, 777, 744, 696, 594, 502 cm^{-1}. Anal. Calcd for $C_{43}H_{63}ClO_{17.5}P_3RuSi_9$[47] (idealized stoichiometry): C, 38.19; H, 5.44; Cl, 2.62; Ru, 7.48. Corrected stoichiometry:[48] C, 36.99; H, 5.62; Cl, 2.54; Ru, 7.24. Found: C, 35.09; H, 5.98; Cl, 2.49; Ru, 7.10.

Carbonylchlorohydridotris[(2-methoxyethyl)phenyl(polysiloxanylpropyl)phosphine-*P,P′,P″*]ruthenium(II) $\mathbf{(T^m)_{12}}$ [$\mathbf{2(T^n)_3(T^m)_{12}}$]. A mixture of $HRuCl(CO)(P{\sim}O)_3$ [$\mathbf{2(T^0)_3}$] (439 mg, 0.379 mmol), 12 equiv of $MeSi(OMe)_3$ ($\mathbf{T^0}$, 619 mg, 4.548 mmol), water (184 mg, 10.23 mmol), and $(n\text{-}Bu)_2Sn(OAc)_2$ (18 mg, 0.05 mmol) was sol–gel processed to give a slightly yellow gel. [$\mathbf{2(T^n)_3(T^m)_{12}}$, 671 mg, 101%]: ^{31}P CP MAS NMR δ 16.4 (P^2), −1.3 (P^1); ^{29}Si CP MAS NMR (silicon substructure) δ −48.8 (T^1), −58.0 (T^2), −64.9 (T^3); IR (KBr) 3434, 3058, 2967, 2931, ν(CO) 1919, 1436, 1272, 1111, 1024, 779, 697, 596, 502 cm^{-1}. Anal. Calcd for $C_{49}H_{91}ClO_{26.5}P_3RuSi_{15}$[47] (idealized stoichiometry): C, 33.53; H, 5.22; Cl, 2.02; Ru, 5.76. Corrected stoichiometry:[48] C, 32.44; H, 5.36; Cl, 1.95; Ru, 5.76. Found: C, 31.27; H, 5.55; Cl, 1.91; Ru, 5.45.

Carbonylchlorohydridotris[(2-methoxyethyl)phenyl(polysiloxanylpropyl)phosphine-*P,P′,P″*]ruthenium(II) $\mathbf{(T^m)_{18}}$ [$\mathbf{2(T^n)_3(T^m)_{18}}$]. A mixture of $HRuCl(CO)(P{\sim}O)_3$ [$\mathbf{2(T^0)_3}$] (240 mg, 0.207 mmol), 18 equiv of $MeSi(OMe)_3$ ($\mathbf{T^0}$ 507 mg, 3.726 mmol), water (141 mg, 7.82 mmol), and $(n\text{-}Bu)_2Sn(OAc)_2$ (14 mg, 0.04 mmol) was sol–gel processed to give a slightly yellow gel. [$\mathbf{2(T^n)_3(T^m)_{18}}$, 360 mg, 81%]: ^{31}P CP MAS NMR δ 16.4 (P^2), −1.7 (P^1); ^{29}Si CP MAS NMR (silicon substructure) δ −49.5 (T^1), −57.0 (T^2), −64.9 (T^3); IR (KBr) 3409, 3057, 2973, 2842, ν(CO) 1919, 1437, 1275, 1114, 1017, 852, 779, 695, 596, 502 cm^{-1}. Anal. Calcd for $C_{55}H_{109}ClO_{35.5}P_3RuSi_{21}$[47] (idealized stoichiometry): C, 30.61; H, 5.09; Cl, 1.64; Ru, 4.69. Corrected stoichiometry:[48] C, 29.66; H, 5.28; Cl, 1.59; Ru, 4.54. Found: C, 27.72; H, 5.76; Cl, 1.29; Ru, 4.24.

Carbonylchlorohydridotris[(2-methoxyethyl)phenyl(polysiloxanylpropyl)phosphine-*P,P′,P″*]ruthenium(II) $\mathbf{(T^m)_{24}}$ [$\mathbf{2(T^n)_3(T^m)_{24}}$]. A mixture of $HRuCl(CO)(P{\sim}O)_3$ [$\mathbf{2(T^0)_3}$] (377 mg, 0.326 mmol), 24 equiv of $MeSi(OMe)_3$ ($\mathbf{T^0}$, 1.064 g, 7.824 mmol), water (285 mg, 15.84 mmol), and $(n\text{-}Bu)_2Sn(OAc)_2$ (21 mg, 0.06 mmol) was sol–gel processed to give a slightly yellow gel. [$\mathbf{2(T^n)_3(T^m)_{24}}$, 813 mg, 98%]: ^{31}P CP MAS NMR δ 15.7 (P^2), −2.1 (P^1); ^{29}Si CP MAS NMR (silicon substructure) δ −48.4 (T^1), −57.2 (T^2), −65.0 (T^3); IR (KBr) 3435, 3057, 2969, 2841, ν(CO) 1924, 1437, 1275, 1118, 1024, 854, 779, 694, 593, 502 cm^{-1}. Anal. Calcd for $C_{61}H_{127}ClO_{44.5}P_3RuSi_{27}$[47] (idealized stoichiometry): C, 28.61; H, 5.00; Cl, 1.38; Ru, 3.95. Corrected stoichiometry:[48] C, 27.70; H, 5.20; Cl, 1.34; Ru, 3.82. Found: C, 25.81; H, 5.65; Cl, 1.15; Ru, 3.29.

Carbonylchlorohydridotris[(2-methoxyethyl)phenyl(polysiloxanylpropyl)phosphine-*P,P′,P″*]ruthenium(II) $\mathbf{(T^m)_{48}}$ [$\mathbf{2(T^n)_3(T^m)_{48}}$]. A mixture of $HRuCl(CO)(P{\sim}O)_3$ [$\mathbf{2(T^0)_3}$] (245 mg, 0.212 mmol), 48 equiv of $MeSi(OMe)_3$ ($\mathbf{T^0}$, 1.384 g, 10.176 mmol), water (352 mg, 19.5 mmol), and $(n\text{-}Bu)_2Sn(OAc)_2$ (25 mg, 0.07 mmol) was sol–gel processed to give a slightly yellow gel. [$\mathbf{2(T^n)_3(T^m)_{48}}$, 798 mg, 90%]: ^{31}P CP MAS NMR δ 15.8 (P^2), −1.0 (P^1); ^{29}Si CP MAS NMR (silicon substructure) δ −49.2 (T^1), −57.0 (T^2), −64.9 (T^3); IR (KBr) 3446, 2973, ν(CO) 1925, 1437, 1276, 1129, 1024, 850, 780, 696, 595, 502 cm^{-1}. Anal. Calcd for $C_{85}H_{199}ClO_{80.5}P_3RuSi_{51}$[47] (idealized stoichiometry): C, 24.47; H, 4.81; Cl, 0.85; Ru, 2.42. Corrected stoichiometry:[48] C, 23.60; H, 5.04; Cl, 0.82; Ru, 2.34. Found: C, 21.69; H, 5.16; Cl, 0.88; Ru, 2.51.

Carbonylchlorohydridotris[(2-methoxyethyl)phenyl(polysiloxanylpropyl)phosphine-*P,P′,P″*]ruthenium(II) $\mathbf{(T^m)_{96}}$ [$\mathbf{2(T^n)_3(T^m)_{96}}$]. A mixture of $HRuCl(CO)(P{\sim}O)_3$ [$\mathbf{2(T^0)_3}$] (178 mg, 0.154 mmol), 96 equiv of $MeSi(OMe)_3$ ($\mathbf{T^0}$, 2.011 g, 14.784 mmol), water (494 mg, 27.4 mmol), and $(n\text{-}Bu)_2Sn(OAc)_2$

---

(43) Stejskal, E. O.; Schaefer, J.; Sefcik, M. D.; McKay, R. A. *Macromolecules* **1981**, *14*, 275.

(44) McBrierty, V. J.; Douglass, D. C.; Kwei, T. K. *Macromolecules* **1978**, *11*, 1265.

(45) McBrierty, V. J.; Douglass, D. C. *J. Polym. Sci., Macromol. Rev.* **1981**, *16*, 295.

(46) Torchia, A. D. *J. Mag. Reson.* **1978**, *30*, 613.

(47) The broken numbers in the chemical formulas are due to $SiO_{3/2}$ units or to the amount of T or D silicon units.

(48) The corrected stoichiometry was obtained by adding the additional number of OH units of the T^1, T^2, and D^1 groups (obtained from the ^{29}Si CP MAS NMR spectra) to the idealized stoichiometry (only T^3 and D^2 units).

(30 mg, 0.09 mmol) was sol−gel processed to give a nearly colorless gel. [**2(T^n)$_3$(T^m)$_{96}$**, 1.1 g, 93%]: ^{31}P CP MAS NMR δ 16.4 (P^2), −1.3 (P^1); ^{29}Si CP MAS NMR (silicon substructure) δ −49.5 (T^1), −56.7 (T^2), −64.9 (T^3); IR (KBr) 3444, 2973, ν(CO) 1925, 1437, 1276, 1129, 1033, 856, 782, 694 cm^{-1}. Anal. Calcd for $C_{133}H_{343}ClO_{152.5}P_3RuSi_{99}$[47] (idealized stoichiometry): C, 21.60; H, 4.68; Cl, 0.48; Ru, 1.37. Corrected stoichiometry: [48] C, 20.83; H, 4.91; Cl, 0.46; Ru, 1.32. Found: C, 20.47; H, 4.98; Cl, 0.43; Ru, 1.30.

Polymethylsiloxane [(T$^m_{PMS}$)$_y$]. A mixture of MeSi(OMe)$_3$ (**T^0**, 2.00 g, 14.71 mmol), water (476 mg, 26.47 mmol), and (n-Bu)$_2$Sn(OAc)$_2$ (30 mg, 0.09 mmol) was sol−gel processed to give colorless polymethylsiloxane **(T$^m_{PMS}$)$_y$**. [**(T$^m_{PMS}$)$_y$**, 1.7 g, 96%]: ^{29}Si CP MAS NMR (silicon substructure) δ −48.9 (T^1), −57.3 (T^2), −64.9 (T^3); IR (KBr) 3443, 2976, 1275, 1125, 1025, 855, 781, 695 cm^{-1}. Anal. Calcd for $CH_3O_{1.5}Si$[47] (idealized stoichiometry): C, 17.89; H, 4.50. Corrected stoichiometry:[48] C, 17.20; H, 4.76. Found: C, 15.82; H, 4.82.

Method 1. 1(T^n)(D^i)$_{1.5}$ and 2(T^n)$_3$(D^i)$_{4.6}$. The ether−phosphine ligand **1(T^0)** or HRuCl(CO)(P∼O)$_3$ **[2(T^0)$_3$]** was dispersed in a mixture of (n-Bu)$_2$Sn(OAc)$_2$, the specified quantity of water, and Me$_2$Si(OEt)$_2$ **(D^0)** and was stirred vigorously in a sealed Schlenk tube at room temperature. Homogenization and solidification takes place after 5 min **[2(T^0)$_3$]** or 8 h **[1(T^0)]**. Methanol and ethanol were pumped off and the residue was placed on a paper filter. The gel was washed with n-hexane (200 mL) and dried under vacuum. The obtained powder was dissolved in 100 mL of toluene and was stirred for 30 min. The polysiloxane precipitated again on adding slowly 100 mL of n-hexane. This procedure was repeated two times to remove oligomeric units of the polysiloxane. Finally the gel was dried 4 h under vacuum at 60 °C.

(2-Methoxyethyl)phenyl(polysiloxanylpropyl)phosphine(D^i)$_{1.5}$ [1(T^n)(D^i)$_{1.5}$]. A mixture of the O,P ligand **1(T^0)** (432 mg, 1.309 mmol), 2 equiv of Me$_2$Si(OEt)$_2$ (**D^0** 388 mg, 2.618 mmol), water (99 mg, 5.5 mmol), and (n-Bu)$_2$Sn(OAc)$_2$ (32 mg, 0.09 mmol) was sol−gel processed to give a colorless rubber. After solvent processing and aging a white powder was formed. [**1(T^n)(D^i)$_{1.5}$**, 310 mg, 58%]: ^{29}Si CP MAS NMR (silicon substructure) δ −6.0 (D^0), −13.8 (D^1), −21.4 (D^2), −59.1 (T^2), −68.3 (T^3); IR (KBr) 3449, 2962, 2934, 2900, 1439, 1264, 1186, 1108, 1015, 804, 744 cm^{-1}. Anal. Calcd for $C_{15}H_{27}O_4PSi_{2.5}$:[47] C, 48.39; H, 7.31. Found: C, 44.90; H, 7.32.

Carbonylchlorohydridotris[(2-methoxyethyl)phenyl(polysiloxanylpropyl)phosphine-*P*,*P*′,*P*″]ruthenium(II) (D^i)$_{4.6}$ [2(T^n)$_3$(D^i)$_{4.6}$]. A mixture of HRuCl(CO)(P∼O)$_3$ **[2(T^0)$_3$]** (585 mg, 0.509 mmol), 6 equiv of Me$_2$Si(OEt)$_2$ (**D^0**, 452 mg, 3.054 mmol), water (115 mg, 6.41 mmol), and (n-Bu)$_2$Sn(OAc)$_2$ (35 mg, 0.1 mmol) was sol−gel processed to give a slightly yellow gel. [**2(T^n)$_3$(D^i)$_{4.6}$**, 605 mg, 85%]: ^{29}Si CP MAS NMR (silicon substructure) δ −6.6 (D^0), −14.2 (D^1), −21.4 (D^2), −49.4 (T^1), −59.2 (T^2), −67.6 (T^3); ^{13}C CP MAS NMR (TOSS, 3.3 kHz) δ 137.1 (C-*i*), 128.6 (C-*o*, -*m*, -*p*), 68.8 (C-5), 58.7 (C-6), 27.6 (C-3, 4), 17.9 (C-2), 14.5 (C-1), −1.2 (SiCH$_3$); IR (KBr) 3408, 3075, 2962, 2927, ν(CO) 1919, 1435, 1261, 1170, 1097, 1018, 845, 800, 744, 694, 594, 501 cm^{-1}. Anal. Calcd for $C_{46.2}H_{82.6}ClO_{13.1}P_3RuSi_{7.6}$:[47] C, 42.99; H, 6.45; Cl, 2.75; Ru, 7.83. Found: C, 43.29; H, 7.07; Cl, 2.56; Ru, 7.48.

Method 2. 2(T^n)$_3$(T$^m_{PMS}$)$_y$ (y = 18). The polysiloxane-bound ruthenium complex HRuCl(CO)(P∼O)$_3$ **[2(T^n)$_3$]** (355 mg, 0.374 mmol), 18 equiv of MeSi(OMe)$_3$ (**T^0**, 915 mg, 6.73 mmol), water (218 mg, 12.1 mmol), and (n-Bu)$_2$Sn(OAc)$_2$ were mixed and polycondensated in a sealed Schlenk tube. After 2 h methanol and ethanol were removed under vacuum and the mixture was worked up according to method 1. ^{29}Si CP MAS NMR (silicon substructure) δ −49.2 (T^1), −57.0 (T^2), −64.9 (T^3). Anal. Calcd for $C_{55}H_{109}ClO_{75.5}P_3RuSi_{21}$[47] (idealized stoichiometry): C, 30.61; H, 5.09; Cl, 1.64; Ru, 4.68. Corrected stoichiometry:[48] C, 29.79; H, 5.25; Cl, 1.60; Ru, 4.56. Found: C, 28.81; H, 5.83; Cl, 1.42; Ru, 4.27.

Method 3. 3(T^n)$_2$(D^i)$_y$ (y = 1.8, 2.4, 2.7). The oily palladium complex PdCl$_2$(P∼O)$_2$ **[3(T^0)$_2$]** was dissolved in a minimum amount of methanol (5 mL). Water, (n-Bu)$_2$Sn(OAc)$_2$, and Me$_2$Si(OEt)$_2$ **(D^0)** were added during stirring. After 1 day the solvent was evaporated and the brittle particles were stirred in 10 mL of n-hexane overnight. After removal of the solvent the complexes were washed with 10 mL of methanol and three times with toluene:n-hexane 1:10. Finally the polysiloxane supported palladium complexes were dried 4 h under vacuum at 40 °C.

Dichlorobis(2-methoxyethyl)phenyl(polysiloxanylpropyl)phosphinepalladium(II) (D^i)$_{1.8}$ [3(T^n)$_2$(D^i)$_{1.8}$]. A mixture of PdCl$_2$(P∼O)$_2$ **[3(T^0)$_2$]** (438 mg, 0.522 mmol), 4 equiv of Me$_2$Si(OEt)$_2$ (**D^0**, 296.6 mg, 2.0 mmol), water (157.5 mg, 8.7 mmol), and (n-Bu)$_2$Sn(OAc)$_2$ (17 mg, 0.05 mmol) was sol−gel processed to give a slightly yellow gel. [**3(T^n)$_2$(D^i)$_{1.8}$**, 400 mg, 92%]: ^{31}P CP MAS NMR δ 8.5 (*trans*), 22.1 (*cis*); ^{29}Si CP MAS NMR (silicon substructure) δ −13.3 (D^1), −21.7 (D^2), −59.2 (T^2), −68.1 (T^3); ^{13}C CP MAS NMR (TOSS, 3.3 kHz) δ 129.7 (C-*i*, -*o*, -*m*, -*p*), 67.9 (C-5), 58.3 (C-6), 30 −12 (C-1, 2, 3, 4), 1.1 (SiCH$_3$); IR (KBr) 3406, 3072, 2960, 2929, 1430, 1250, 1170, 1092, 1017, 841, 799, 742, 694, 503 cm^{-1}. Anal. Calcd for $C_{27.6}H_{46.8}Cl_2O_{6.8}P_2PdSi_{3.8}$:[47] C, 39.78; H, 5.66; Cl, 8.51; Pd, 12.77. Found: C, 35.38; H, 5.89; Cl, 7.99; Pd, 11.94.

Dichlorobis(2-methoxyethyl)phenyl(polysiloxanylpropyl)phosphinepalladium(II) (D^i)$_{2.4}$ [3(T^n)$_2$(D^i)$_{2.4}$]. A mixture of PdCl$_2$(P∼O)$_2$ **[3(T^0)$_2$]** (469.6 mg, 0.560 mmol), 8 equiv of Me$_2$Si(OEt)$_2$ (**D^0** 664 mg, 4.48 mmol), water (277.2 mg, 15.4 mmol), and (n-Bu)$_2$Sn(OAc)$_2$ (35 mg, 0.1 mmol) was sol−gel processed to give a slightly yellow gel. [**3(T^n)$_2$(D^i)$_{2.4}$**, 392 mg, 80%]: ^{31}P CP MAS NMR δ 8.4 (*trans*), 22.0 (*cis*); ^{29}Si CP MAS NMR (silicon substructure) δ −13.3 (D^1), −21.7 (D^2), −59.2 (T^2), −68.1 (T^3); ^{13}C CP MAS NMR (TOSS, 3.3 kHz) δ 129.8 (C-*i*, -*o*, -*m*, -*p*), 67.8 (C-5), 58.2 (C-6), 30 − 14 (C-1, 2, 3, 4), 1.1 (SiCH$_3$); IR (KBr) 3405, 3074, 2964, 2930, 1435, 1261, 1172, 1096, 1019, 843, 775, 742, 694, 502 cm^{-1}. Anal. Calcd for $C_{28.8}H_{50.4}Cl_2O_{7.4}P_2PdSi_{4.4}$:[47] C, 39.40; H, 5.64; Cl, 7.87; Pd, 12.11. Found: C, 35.96; H, 6.21; Cl, 6.91; Pd, 11.34.

Dichlorobis(2-methoxyethyl)phenyl(polysiloxanylpropyl)phosphinepalladium(II) (D^i)$_{2.7}$ [3(T^n)$_2$(D^i)$_{2.7}$]. A mixture of PdCl$_2$(P∼O)$_2$ **[3(T^0)$_2$]** (503 mg, 0.600 mmol), 16 equiv of Me$_2$Si(OEt)$_2$ (**D^0**, 1.42 g, 9.6 mmol), water (504 mg, 28 mmol), and (n-Bu)$_2$Sn(OAc)$_2$ (35 mg, 0.1 mmol) was sol−gel processed to give a slightly yellow gel. [**3(T^n)$_2$(D^i)$_{2.7}$**, 378 mg, 70%]: ^{31}P CP MAS NMR δ 8.1 (*trans*), 21.8 (*cis*); ^{29}Si CP MAS NMR (silicon substructure) δ −13.4 (D^1), −21.7 (D^2), −59.5 (T^2), −68.5 (T^3); ^{13}C CP MAS NMR (TOSS, 3.3 kHz) δ 130.7 (C-*i*, -*o*, -*m*, -*p*), 67.8 (C-5), 58.3 (C-6), 30 − 14 (C-1, 2, 3, 4), 1.1 (SiCH$_3$); IR (KBr) 3405, 3071, 2970, 2925, 1432, 1248, 1180, 1095, 1017, 841, 800, 744, 696, 501 cm^{-1}. Anal. Calcd for $C_{29.4}H_{52.2}Cl_2O_{7.7}P_2PdSi_{4.7}$:[47] C, 39.22; H, 5.84; Cl, 7.88; Pd, 11.88. Found: C, 36.25; H, 6.12; Cl, 6.20; Pd, 10.45.

Acknowledgment. The support of this research by the Deutsche Forschungsgemeinschaft (Forschergruppe, Grant No. Li 154/41-1) Bonn/Bad Godesberg, and by the Fonds der Chemischen Ind., Frankfurt/Main is gratefully acknowledged. We are grateful to Degussa AG, Germany for a generous gift of PdCl$_2$. R.S. thanks the Land Baden-Württemberg and the University of Tübingen for a scholarship (Landesgraduiertenförderungsgesetz).

CM9405537